

Radiative and conductive transfer for a real gas in a cylindrical enclosure with gray walls

T. K. KIM and T. F. SMITH

Department of Mechanical Engineering, University of Iowa, Iowa City, IA 52242, U.S.A.

(Received 27 November 1984 and in final form 10 June 1985)

Abstract—The purpose of this study is to examine the interaction of radiative and conductive transfer for a radiatively participating real gas stagnant in a cylindrical enclosure with gray diffuse walls. Consideration of reflecting boundaries represents an extension of previous black wall studies. Examination of radiative transfer was made by the zone method with gas radiative properties furnished by the weighted sum of gray gases model. Directed flux areas are expressed as the weighted sum of gray gas total exchange areas which are evaluated using the matrix formulation method from direct exchange areas. Axial and radial gas temperatures are examined along with wall heat flux or temperature for respective cases of either specified wall temperatures or heat fluxes. Emphasis is placed on examining results to show the effects of wall emittance and duct diameter. Results for heat generation within the gas are also presented.

INTRODUCTION

EXAMINATION of radiative heat transfer in a circular enclosure involving flow of a gas has been performed because of its wide applications to such systems as combustion chambers and furnaces. However, adequate two-dimensional heat transfer studies for systems containing stagnant real gases are lacking. Such systems occur when the process producing the gas movement is interrupted, or in nuclear reactor enclosures filled with steam. In most of these systems, the walls are not black but may be coated with deposits or may be exposed metal. Thus, there is need for additional studies on enclosures where the reflection from enclosure walls is accounted for.

There are at least two distinct methods of approach to describe radiative transport in the presence of a participating medium. One is developed starting with the radiant transport equation, introduces band correlation models such as those developed by Edwards [1], and uses integrals to describe radiative transport. The other method called the zone method is oriented toward engineering analysis and is based mainly on the work of Hottel and co-workers [2, 3]. The zone method is widely accepted for applications in energy generation systems [4–16] because of its ability to include real gas and gray wall conditions and to yield results for multidimensional analyses. Thus, the zone method is adopted for this investigation.

The purpose of the present study is to analyze energy transport mechanisms occurring within a system where two-dimensional radiant transport analysis is included along with reflecting boundaries. Results sought consist of axial and radial temperature profiles within the gas and heat flux or temperature distributions of surrounding surfaces for various values of the governing parameters. The present analysis and results could form the basis for a study involving fluid flow.

ANALYSIS

System description

The system chosen for this study consists of a stagnant gas within a circular duct of diameter D and length L . The gas is assumed to be uniform in composition, to be isobaric, to have a refractive index of unity, and to have attained the steady-state condition. The gas emits and absorbs radiant energy, and in the absence of suspended particles in the gas, radiation scattering is neglected. Axial and radial components of heat conduction are considered and a constant thermal conductivity is specified for the gas. A volumetric heat source may be distributed within the gas in order to simulate additional heat sources. The surfaces are assumed to be gray, diffuse emitters and reflectors of radiant energy and are opaque. Axial conduction within the wall surface could be included but is neglected since it has been shown to be negligible [13, 17]. The wall surface may either assume a prescribed temperature or heat flux distribution. For reference purposes, the end surfaces at $x = 0$ and $x = L$ are called the inlet and outlet ends, respectively. The inlet and outlet ends are maintained at prescribed temperature distributions.

Application of zone method

With the zone method of analysis, the cylindrical enclosure is subdivided into a number of volume and surface zones where each zone is isothermal with uniform properties. The gas is divided into volume zones with radial width $B = D/2N$ and axial length $H = L/M$ where N and M denote the number of radial and axial zones, respectively. Subscripts (i, j) refer to the zone under consideration and (k, l) are for the zones contributing radiant energy to (i, j) . The first (i or k) and second (j or l) subscripts identify the radial and

NOMENCLATURE

a_e	weighting factors for emissivity
A	surface area [m ²]
B	radial zone width [m]
c	coefficient in equation (12)
D	diameter of the duct [m]
e	coefficient in equation (12)
EE	end to end total exchange area
$\overrightarrow{EE}, \overrightarrow{EG}, \overrightarrow{EW}$	end to end, end to gas, and end to wall directed flux areas
GG, GS	gas to gas and gas to surface total exchange areas
$\overrightarrow{GG}, \overrightarrow{GS}, \overrightarrow{GW}$	gas to gas, gas to surface, and gas to wall directed flux areas
H	axial zone width [m]
k_g	thermal conductivity of gas [W m ⁻¹ K ⁻¹]
L	length of tube [m]
M	number of axial zones, L/H
N	number of radial zones, $D/2B$
N_g	number of gray gases
\bar{N}_g	gas conduction-radiation parameter, $k_g \kappa_{T,r}/4\sigma T_r^3$
P	pressure [atm]
\dot{q}	volumetric heat generation [W m ⁻³]
q^c	net conductive transfer [W]
q^r	radiant energy absorbed by the volume zone [W m ⁻³]
q_w^r	radiant energy absorbed by the wall zone [W m ⁻²]
\dot{Q}	dimensionless heat generation, $\dot{q}D/\sigma T_r^4$
Q	dimensionless heat flux at the surface, $q''/\sigma T_r^4$
Q^c	dimensionless conductive transfer to the volume zone, $q^c H/k_g \pi B^2 T_r$
Q_w^c	dimensionless conductive transfer to the wall zone, $q^c/\pi B^2 \sigma T_r^4$
Q^r	dimensionless radiant energy absorbed by the volume zone, $q^r/4\kappa_T \sigma T_r^4$
Q_w^r	dimensionless radiant energy absorbed by the wall zone, $q_w^r/\pi B^2 \sigma T_r^4$
SG, SS	surface to gas and surface to surface total exchange areas

$\overrightarrow{SG}, \overrightarrow{SS}$	surface to gas and surface to surface directed flux areas
T	temperature [K]
V	volume [m ³]
$\overrightarrow{WG}, \overrightarrow{WW}$	wall to gas and wall to wall directed flux areas
x	axial distance [m].

Greek symbols

β	relaxation factor
ε	emittance
ζ	ratio of length to diameter, L/D
η	ratio of axial to radial zone width, H/B
θ	dimensionless temperature, T/T_r
κ	absorption coefficient [m ⁻¹]
σ	Stefan-Boltzmann constant, [W m ⁻² K ⁻⁴]
τ	optical thickness, $\kappa_T D$.

Matrix notations

C	coefficient matrix in equation (13)
E	coefficient matrix in equation (13)
gg, gs	gas to gas and gas to surface direct exchange area matrices
GG, GS	gas to gas and gas to surface total exchange area matrices
sg, ss	surface to gas and surface to surface direct exchange area matrices
SG, SS	surface to gas and surface to surface total exchange area matrices
χ	defined by equation (10).

Subscripts

e	inlet
g	gas
o	outlet
r	reference
T	total
w	wall.

Superscripts

m	iteration number
T	transpose.

axial zone locations, respectively. For an end zone, only a single subscript related to its radial position is assigned. Likewise, for a wall zone, the single subscript describes the axial location of the zone.

Governing equations

Energy balance. The energy balance for a volume

zone $V_{i,j}$ is written as

$$4\kappa_{T,i,j}V_{i,j}\sigma T_{g,i,j}^4 - q_{i,j}^rV_{ij} = q_{i,j}^c + \dot{q}_{i,j}V_{i,j} \tag{1}$$

where the total absorption coefficient κ_T is evaluated at the zone temperature $T_{i,j}$, q^r is the volumetric rate at which radiant energy is absorbed by the zone, q^c is the net conductive heat transfer to the zone, and \dot{q} is the

volumetric heat generation. By introducing a reference temperature T_r , dimensionless temperature $\theta = T/T_r$, and dimensionless parameters and variables, equation (1) transforms to

$$Q_{i,j}^c = \frac{(2i-1)\zeta^2\tau_r\tau_{i,j}}{M^2\bar{N}_g}\theta_{g,i,j}^4 = \frac{(2i-1)\zeta^2\tau_r}{M^2\bar{N}_g}\left(-\tau_{i,j}Q_{i,j}^r - \frac{Q_{i,j}}{4}\right) \quad (2)$$

where \bar{N}_g is the gas conduction to radiation parameter based on T_r . τ is the optical thickness where subscripts (i, j) and r indicate that it is evaluated at $T_{i,j}$ and T_r , respectively.

An energy balance for a wall zone $A_{w,j}$ is stated in dimensionless form as

$$\varepsilon_{w,j}\theta_{w,j}^4 - \frac{Q_{w,j}^r}{2N\eta} - \frac{Q_{w,j}^c}{2N\eta} - Q_{w,j} = 0. \quad (3)$$

In the above equation, the first term is the wall zone emission with ε_w denoting the wall emittance, Q_w^r denotes the radiant energy absorbed by the wall zone, and Q_w^c represents the radial conduction from the adjacent volume zone. The last term is the imposed wall zone heat flux when θ_w is sought or is the resulting wall heat flux when θ_w is prescribed. Further explanation for Q^r and Q^c in the energy balances is required and given in the following discussion. An energy balance for an end zone can be written in a similar manner as that for a wall zone [17] and is not presented here.

Radiant energy. The dimensionless radiant energy absorbed for a volume zone is written as

$$Q_{i,j}^r = \frac{M}{4(2i-1)\zeta\tau_{i,j}} \left[\sum_{k=1}^N (\overrightarrow{E_{e,k}} G_{i,j}\theta_{e,k}^4 + \overrightarrow{E_{o,k}} G_{i,j}\theta_{o,k}^4) + \sum_{l=1}^M \overrightarrow{W_l} G_{i,j}\theta_{w,l}^4 + \sum_{k=1}^N \sum_{l=1}^M \overrightarrow{G_{k,l}} G_{i,j}\theta_{g,k,l}^4 \right]. \quad (4)$$

Directed flux areas for end to gas, wall to gas, and gas to gas radiant energy exchanges are represented, respectively, by \overrightarrow{EG} , \overrightarrow{WG} , and \overrightarrow{GG} .

The radiant energy absorbed by a wall zone is expressed by

$$Q_{w,j}^r = \sum_{k=1}^N (\overrightarrow{E_{e,k}} \overrightarrow{W_j} \theta_{e,k}^4 + \overrightarrow{E_{o,k}} \overrightarrow{W_j} \theta_{o,k}^4) + \sum_{l=1}^M \overrightarrow{W_l} \overrightarrow{W_j} \theta_{w,l}^4 + \sum_{k=1}^N \sum_{l=1}^M \overrightarrow{G_{k,l}} \overrightarrow{W_j} \theta_{g,k,l}^4. \quad (5)$$

End to wall, wall to wall, and gas to wall directed flux areas are represented by \overrightarrow{EW} , \overrightarrow{WW} , and \overrightarrow{GW} , respectively. In equations (4) and (5), directed flux areas have been normalized with the factor πB^2 as found convenient [18]. The arrow over the directed flux areas indicates the direction in which radiant energy travels. Specification of the directed flux areas is given later.

Conduction. Conductive transfer terms for volume zones are written in terms of dimensionless variables as

$$Q_{i,j}^c = 2i\eta^2(\theta_{g,i+1,j} - \theta_{g,i,j}) + 2(i-1)\eta^2(\theta_{g,i-1,j} - \theta_{g,i,j}) + (2i-1)(\theta_{g,i,j-1} + \theta_{g,i,j+1} - 2\theta_{g,i,j}). \quad (6)$$

The first two terms on the RHS account for conductive transfer in the radial direction and the third term represents conduction in the axial direction. Special care must be taken to evaluate the conduction terms for volume zones adjacent to end and wall zones, on the cylindrical axis, and with a radial location of $i = 2$. Specific forms for the conduction terms for these special cases are given elsewhere [17].

The radial conduction from a volume zone adjacent to a wall zone is written as

$$Q_{w,j}^c = \frac{64\bar{N}_g N^3 \zeta}{\tau_r M} (\theta_{g,N,j} - \theta_{w,j}). \quad (7)$$

RADIATION MODEL

Total absorption coefficient

The total absorption coefficient is derived by Smith [19] in terms of the weighted sum of gray gases model and expressed by

$$\kappa_T = \sum_{i=1}^{N_g} a_{e,i}(T) \kappa_i \quad (8)$$

where κ_i are the gray gas absorption coefficients. The temperature dependency of the total emission is given by the emissivity weighting factors $a_{e,i}$ which are generally described in terms of polynomials in temperatures. Reported values [20] for the absorption and polynomial coefficients for carbon dioxide, water vapor and mixtures of these gases are used and consider all absorbing bands for these gases.

Direct exchange areas

Direct exchange areas are fundamental factors for the zone method and, for black surfaces, give the direct radiant exchange between surface zones and/or volume zones. In this study, direct exchange areas developed by Smith *et al.* [18] are used.

Total exchange areas

In an enclosure with gray walls, a portion of the arriving radiation at a zone may have undergone reflection, which contributes to the net radiant energy transport between zones. The multiple reflections are accounted for by the total exchange areas. Four types of total exchange areas associated with surface to surface (SS), surface to gas (SG), gas to surface (GS), and gas to gas (GG) were obtained from the direct exchange areas using the matrix method reported by Noble [21]. For a non-scattering medium, these expressions are given in

matrix form as follows

$$\begin{aligned} \mathbf{SS} &= \boldsymbol{\varepsilon} \mathbf{I} \cdot \mathbf{AI} \cdot \boldsymbol{\chi}^{-1} \cdot \mathbf{ss} \cdot \boldsymbol{\varepsilon} \mathbf{I} \\ \mathbf{SG} &= \boldsymbol{\varepsilon} \mathbf{I} \cdot \mathbf{AI} \cdot \boldsymbol{\chi}^{-1} \cdot \mathbf{sg} = \mathbf{GS}^T \\ \mathbf{GG} &= \mathbf{gg} + \mathbf{gs} \cdot \boldsymbol{\rho} \mathbf{I} \cdot \boldsymbol{\chi}^{-1} \cdot \mathbf{sg} \end{aligned} \quad (9)$$

where $\boldsymbol{\varepsilon}$ and $\boldsymbol{\rho}$ represent surface emittance and reflectance vectors, respectively, and \mathbf{A} is the surface area vector. Surface to surface, surface to gas, gas to surface, and gas to gas direct exchange area matrices are represented by \mathbf{ss} , \mathbf{sg} , \mathbf{gs} and \mathbf{gg} , respectively. \mathbf{I} is the identity matrix. The matrix $\boldsymbol{\chi}$ is defined as

$$\boldsymbol{\chi} = \mathbf{AI} - \mathbf{ss} \cdot \boldsymbol{\rho} \mathbf{I}. \quad (10)$$

The matrix notation for direct and total exchange areas is a generalization of the scalar notation in ref. [3]. The matrix method allows the presence of black surface zones while the scalar method of ref. [3] is restricted to a completely gray enclosure. With the direct exchange areas specified, the total exchange areas take about 50 s on a Prime 850 to evaluate for each gray gas component and surface emittance for a zone pattern where $N = 5$ and $M = 20$.

Directed flux areas

The total radiative exchange between zones is described in terms of the directed flux areas evaluated from the weighted sum of a gray gases model and total exchange areas [17]. Four types of directed flux areas introduced in this investigation are written in a similar manner as that suggested by Smith [19].

$$\begin{aligned} \overrightarrow{G_i S_j} &= \sum_{n=1}^{N_g} a_{e,n}(T_i)(G_i S_j)_n \\ \overrightarrow{S_i G_j} &= \sum_{n=1}^{N_g} a_{z,n}(T_i, T_j)(S_i G_j)_n \\ \overrightarrow{G_i G_j} &= \sum_{n=1}^{N_g} a_{e,n}(T_i)(G_i G_j)_n \\ \overrightarrow{S_i S_j} &= \sum_{n=1}^{N_g} a_{z,n}(T, T_i)(S_i S_j)_n \end{aligned} \quad (11)$$

where, for example, $(G_i S_j)_n$ is the total exchange area for a gray gas with absorption coefficient κ_n . T is some gas temperature whose specific value is not a consequence of the analysis [19] and an average value of gas temperature separating zone areas A_i and A_j was employed.

SOLUTION SCHEME

For a particular location (i, j) , the energy balance can be expressed as

$$\begin{aligned} e_{i,j-1} \theta_{g,i,j-1} + e_{i-1,j} \theta_{g,i-1,j} + e_{i,j} \theta_{g,i,j} \\ + e_{i+1,j} \theta_{g,i+1,j} + e_{i,j+1} \theta_{g,i,j+1} = c_{i,j} \end{aligned} \quad (12)$$

where the coefficients of θ include only the conduction parameters except $e_{i,j}$ which also carries the radiant emission term. The radiant emission has been

linearized [22] as $\theta^4 = \theta_o^3 \theta$ where θ_o is the previous iteration gas temperature at location (i, j) . The advantages of using the linearization technique are that larger relaxation factors can be used, convergence is fast, and computer processor time is saved [16, 22]. This linearization scheme only applies to the numerical solution scheme, and the problem including all nonlinear effects due to large temperature differences is solved in its entirety. For all volume zones, the system of equations is written in the matrix form as

$$\mathbf{E} \cdot \boldsymbol{\theta} = \mathbf{C} \quad (13)$$

where the matrix \mathbf{E} is a function of zone geometry and the linearized radiant emission term and \mathbf{C} includes terms associated with surface conduction, radiant energy absorbed by the gas, and heat generation. The system of equations given by equation (13) has a banded coefficient matrix \mathbf{E} and was solved using an IMSL subroutine [23].

Basically, the solution scheme begins by providing initial estimates for the temperature profiles. The radiant terms are then evaluated and the elements of \mathbf{E} and \mathbf{C} are computed utilizing the required parameters. One of the elements in \mathbf{C} contains the directed flux areas, which are temperature dependent. Thus, the numerical solution technique introduces two iteration schemes, external and internal [17]. The directed flux areas are updated at each external iteration but not at each internal iteration. The new gas temperatures are obtained by solving equation (13). The gas temperatures are then adjusted by a relaxation technique according to the following equation

$$\theta_{i,j}^{m+1} = \theta_{i,j}^m + \beta(\bar{\theta}_{i,j}^{m+1} - \theta_{i,j}^m) \quad (14)$$

where m is the iteration number, β is the relaxation factor, and $\bar{\theta}$ is the temperature evaluated from (13) before relaxation. The updated temperatures are utilized to calculate new radiation terms and to modify subsequently \mathbf{E} and \mathbf{C} . This internal procedure is continued until the differences between successive temperature results are within a relative error of 0.01%. The directed flux areas are then computed and the internal iteration is repeated. The scheme continues until convergence is achieved for both internal and external iterations.

RESULTS AND DISCUSSIONS

The analysis of heat transfer processes within a cylindrical enclosure introduced a radiatively participating stagnant gas introducing several parameters consisting of ζ , \bar{N}_g , ε_e , ε_o , ε_w , \dot{Q} , and gas radiative properties. Results are displayed for a reference temperature of 800 K since the radiant energy terms in the governing equations include the weighting factors represented by polynomials explicitly expressed in terms of the absolute gas temperature. Furthermore, since gas radiative properties are specified for certain ranges of partial pressure–path length product, the cylinder diameter was assigned a value of 1 m with a

larger value of 10 m considered in a limited number of results. The cylinder was chosen to have $\zeta = 5$. The characteristic length of the system is selected as the cylinder diameter. The gas is taken to exist at a total pressure of 1 atm and contains an equimolal mixture of carbon dioxide and water vapor each at a partial pressure of 0.1 atm. The conduction to radiation parameter \bar{N}_g is fixed once the gas species and reference temperature are specified. In this study, a value of $\bar{N}_g = 0.001$ is used. Wall emittance is specified at values from 0.0 to 1.0, and both ends are black. Uniform end and wall temperatures are specified at 1.0 and 2.0, respectively. A dimensionless wall heat flux of 0.5 is prescribed when determining the gas and wall temperatures for specified wall heat flux case. The ranges for these boundary conditions are governed by the temperature range of 600 to 2400 K of available gas radiative properties.

The analysis for demonstrating the effects of the above parameters is performed utilizing five radial and 20 axial zones. Results reported here are in agreement with those for a finer grid [17]. Results for the pure conduction case were computed using the zone method and showed good agreement with those obtained from an analytical solution [17].

Wall emittance effect

Representative results for gas temperature distributions are displayed by three-dimensional diagrams with radial, axial and temperature axes as shown in Fig. 1. The radial axis, r/D , ranges from 0 to 0.5 with the wall located at $r/D = 0.5$. As a result of symmetry the axial axis, x/D , acquires values between 0 and 2.5, with the end located at $x/D = 0$. The zone temperatures were computed for $N = 5$ and $M = 20$. The other temperatures were obtained from a Lagrangian interpolation of these results.

The effect of wall emittance on gas temperatures for specified wall temperatures is illustrated in Fig. 1. Wall emittance varies from 0.01 at the top to 1.0 at the bottom. As ϵ_w increases, the gas temperatures rapidly approach the wall temperatures particularly for $0.01 < \epsilon_w < 0.1$ and are relatively insensitive to wall emittance for $0.5 < \epsilon_w < 1.0$. One interesting observation is that in an enclosure where the optical depth is small, there is negligible absorption of radiant energy within the gas. Since any location within the gas may transfer radiant energy to the surfaces without recourse to the other locations [24], a small temperature gradient exists due to conduction. This observation closely approximates the results in Fig. 2. Thus, the equimolal mixture of carbon dioxide and water vapor is considered to have a small optical depth. The total optical depth ranges from 1.06 to 3.13, which, based on the previous observation, implies an optically thin gas for a real gas. However, these values for optical depth are interpreted as intermediate optical depths for a gray gas.

Representative wall heat flux distributions for conditions identical to those in Fig. 1 are examined by

$$D=1 \text{ m} \quad \bar{N}_g=0.001 \quad T_r=800 \text{ K} \quad P_T=1 \text{ atm} \quad P_w/P_c=1$$

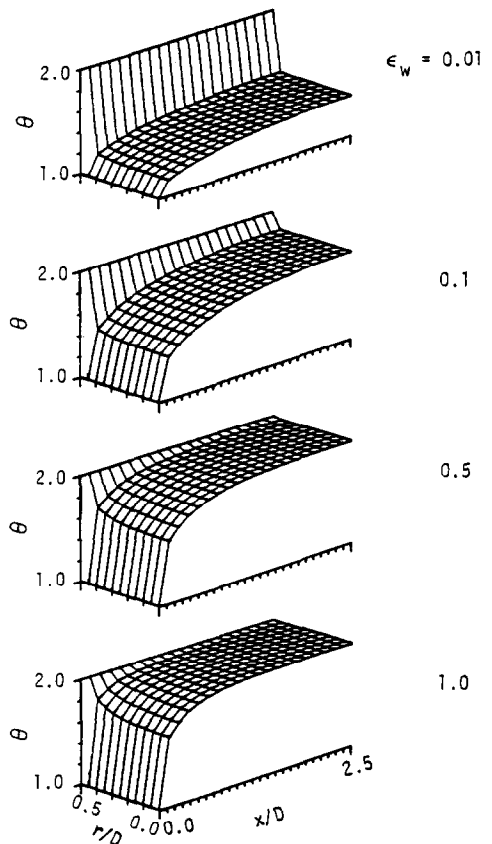


FIG. 1. Effect of wall emittance on gas temperatures.

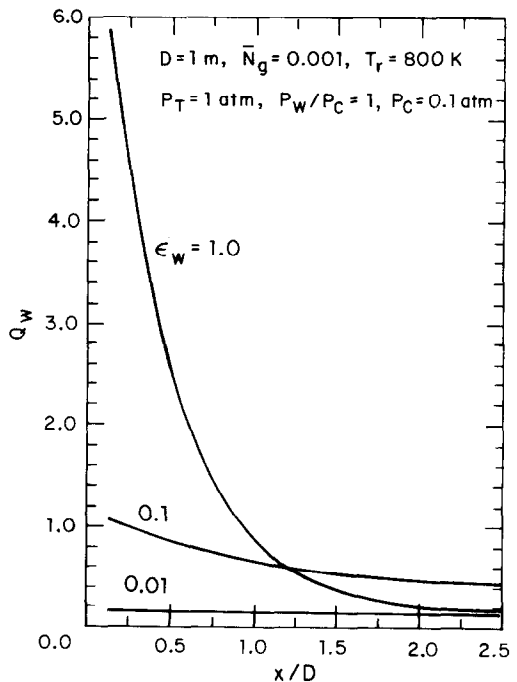


FIG. 2. Wall heat flux results.

reference to Fig. 2. Results for $\epsilon_w = 0.5$ are similar to those for $\epsilon_w = 1.0$ and are not shown. Thus, the effect of ϵ_w is mostly when $\epsilon_w < 0.5$. It is observed that Q_w is nonuniform with the highest values occurring near the end and decreases monotonically along the axial distance until $x/D = 2.5$. The effects of ϵ_w are more clearly shown in Fig. 3 where Q_w results are illustrated as a function of ϵ_w for $x/D = 0.125$ and 2.375 . As ϵ_w decreases, a nearly uniform distribution for Q_w is found. Wall heat fluxes near the end increase as ϵ_w increases and near $x = L/2$ increase as ϵ_w increases from 0.01 to 0.1 but decrease thereafter.

The effect of ϵ_w on the contribution of radiative transfer to the local wall heat flux is presented in Fig. 4 where results are given for the ratio Q_w^r/Q_w . These results are for specified wall heat fluxes where $Q_w = 0.5$. As expected, this ratio increases as ϵ_w increases and the effect of ϵ_w on this ratio is small for $\epsilon_w > 0.5$. Large values of this ratio are obtained even for ϵ_w as low as 0.01 where $Q_w^r/Q_w > 0.9$. Thus, the effect of radiation is important when compared to conduction effects and wall heat fluxes due to conductive transfer are negligible when $\epsilon_w > 0.1$. This is also illustrated by the small value of \bar{N}_g .

Diameter effect

The dependency of gas temperatures and wall heat fluxes on cylinder diameter is illustrated in Figs. 5(a) and (b), respectively, for specified wall temperatures. It should be noted that the duct length also varies as the duct diameter changes to maintain $\zeta = 5$. Results are displayed for diameters of 1 and 10 m where $\epsilon_w = 0.1, 0.5$

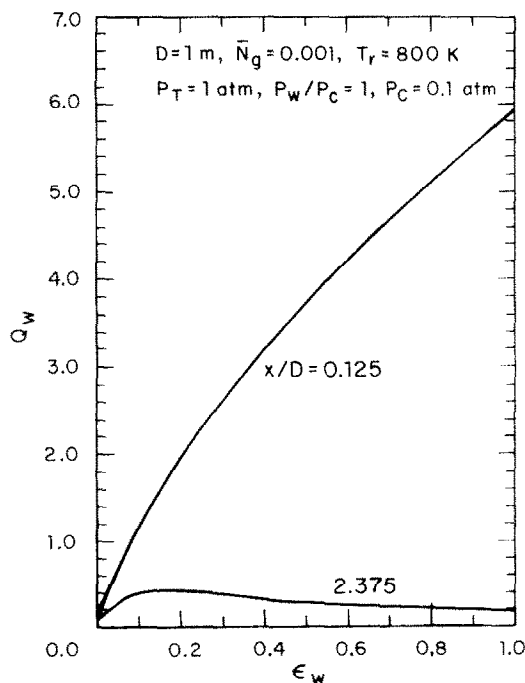


FIG. 3. Effect of wall emittance on wall heat fluxes.

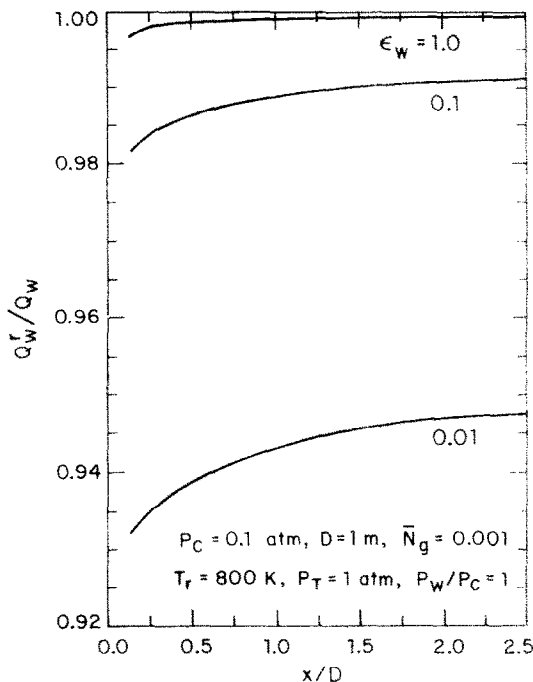


FIG. 4. Contribution of radiative transfer to wall heat fluxes.

and 1.0. Gas temperatures are shown as a function of the radial direction for an axial location of $x/D = 0.125$ where the maximum difference occurs between cases of different diameters. These results show that gas temperatures are not sensitive to diameter. As expected from gas temperature results, wall heat fluxes are not sensitive to diameter, and only a small decrease in wall heat fluxes is observed as the diameter increases. As noted in the previous discussion, the gas is considered to be optically thin which implies that the gas does not absorb its own emission although it absorbs radiant energy emitted by the surrounding surfaces. This is sometimes referred to as negligible self-absorption [24]. Consequently, the gas exchanges radiant energy with the wall without radiative interaction between the gas elements, that is, the wall can see the gas directly. Thus, gas temperatures and wall heat fluxes are not sensitive to diameter.

Heat generation

Gas temperatures with heat generation are presented in Fig. 6 where the radius of the heat generating core is equal to 0.2 of the cylinder radius and the heat generation is uniform within the core which extends the full axial length of the cylinder. Wall and end temperatures are equal to 1.0 with $\dot{Q} = 10$ and 100 for $D = 1$ and 10 m, respectively. The values of \dot{Q} were selected such that the same volumetric heat generation exists for both values of the cylinder diameter. For each \dot{Q} , results for $\epsilon_w = 0.1$ and 1.0 are shown. Results for $\epsilon_w = 0.5$ are similar to those for $\epsilon_w = 1.0$ and, thus, are not shown. The view is through the cylinder from the inlet

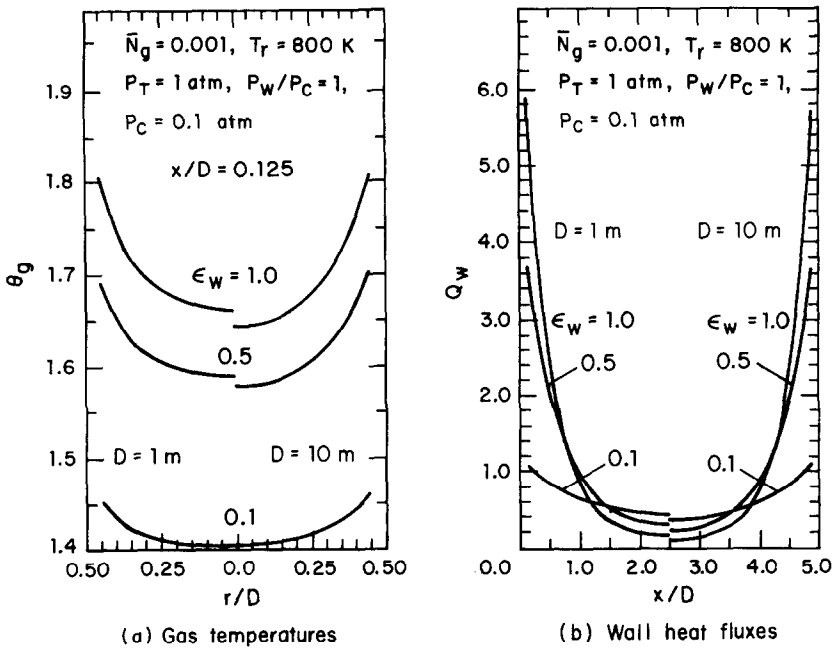


FIG. 5. Diameter effect.

end with the cylinder wall along the axis. Gas temperatures within the heat generating core are higher than those of the surrounding gas. As ϵ_w increases, the entire temperature level in the tube decreases since the radiant energy absorbed by the wall increases, and the axial variation of gas temperatures becomes

more uniform. However, the axial variation of gas temperature is small and significant variation occurs in the radial direction, which indicates that the end effect on gas temperatures is relatively small. The opposite trend for gas temperatures as that with increasing ϵ_w occurs as the diameter increases from 1 to

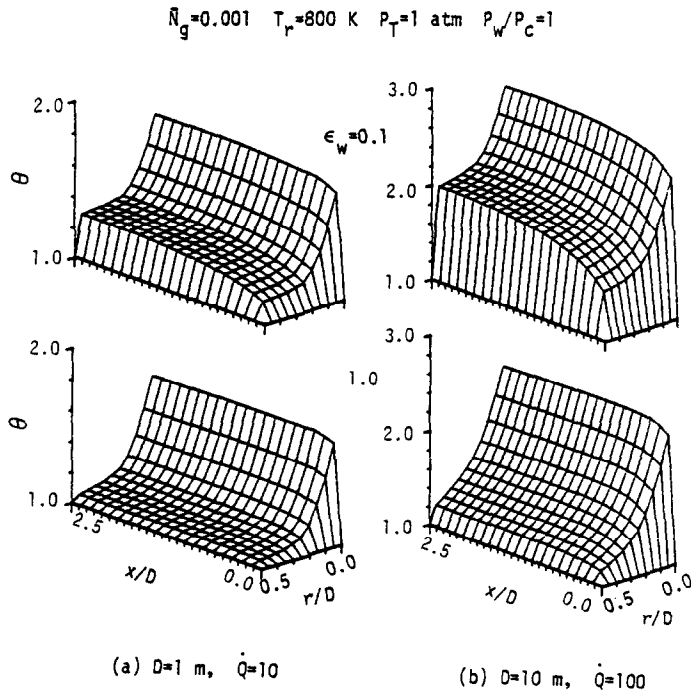


FIG. 6. Gas temperatures for heat generation.

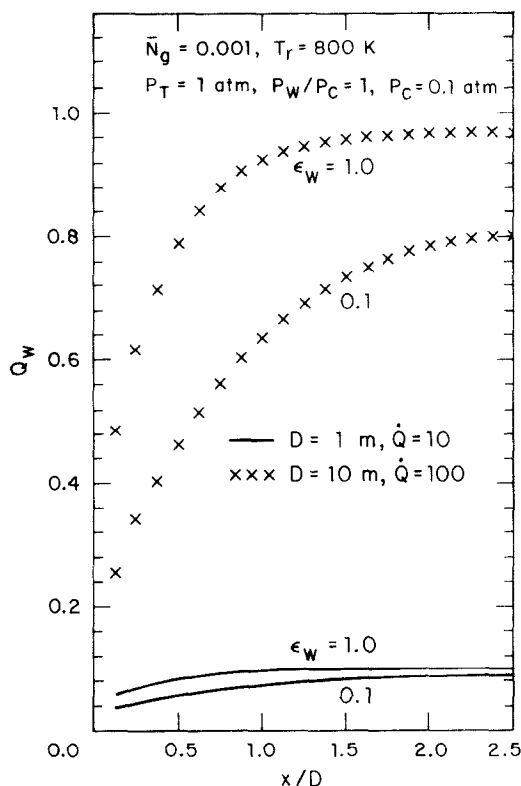


FIG. 7. Wall heat fluxes for heat generation.

10 m. In this study, the ratio of length to diameter is fixed at $\zeta = 5$. Thus, the areas of the surrounding surfaces including the wall and both ends and the total heat generation increase with the second and third power of diameter, respectively. Consequently, the increase of the total heat generation is faster than that of the surface areas, which results in an increase of gas temperatures.

Figure 7 shows wall heat fluxes for the identical parameters as those in Fig. 6. Since energy must be removed from the wall, negative wall heat fluxes are obtained. However, in this figure the absolute values of wall heat fluxes are implied and signified by Q_w . Wall heat fluxes are smallest near the end and increase until $x/D = 2.5$. More uniform wall heat fluxes for $x/D > 1.0$ and steeper increases in wall heat fluxes near the end occur as ϵ_w increases since a smaller portion of the heat generation is removed by the ends. As the diameter increases wall heat fluxes increase significantly since more heat is generated within the core.

CONCLUSIONS

The objective of this study was to examine the interaction of radiative and conductive heat transfer for a radiatively participating real gas stagnant in a gray diffuse wall circular duct. Examination of the radiant exchange in this study was made by the zone method. Total exchange areas were introduced in the expression

for the directed flux areas. Results for specified wall temperatures or heat fluxes are presented with several system variables. Emphasis is placed on examining the influence of wall emittance and duct diameter.

Results for gas temperatures and wall heat fluxes demonstrate that the effect of the wall emittance on these results is significant when wall emittance is less than 0.5. Wall heat fluxes are nonuniform with the highest values occurring near the end and become more uniform as the wall emittance decreases. The effect of radiation on wall heat fluxes is important when compared to conduction effects.

Gas temperatures and wall heat fluxes are not sensitive to diameter since the gas is considered as optically thin. Results for heat generation are presented where the uniform volumetric heat generation exists along the center axis zones. Higher gas temperatures are obtained as wall emittance decreases and/or the diameter increases.

Acknowledgements—The authors gratefully acknowledge the financial assistance of the United States Department of Energy, Grant No. DE-AC02-79ER10515.A000 for partial support of this research. Appreciation is also extended to the University of Iowa for providing computer time.

REFERENCES

1. D. K. Edwards, Molecular gas band radiation, *Adv. Heat Transfer* **12**, 115–193 (1976).
2. H. C. Hottel and E. S. Cohen, Radiant heat exchange in gas filled enclosure: allowance for non-uniformity of gas temperature, *A.I.Ch.E. JI* **4**, 3–14 (1958).
3. H. C. Hottel and A. F. Sarofim, *Radiative Transfer*. McGraw-Hill, New York (1967).
4. T. H. Einstein, Radiant heat transfer to absorbing gases enclosed in a circular pipe with conduction, gas flow and internal heat generation, NASA TR R-156 (1963).
5. H. C. Hottel and A. F. Sarofim, The effect of gas flow patterns on radiative transfer in cylindrical furnaces, *Int. J. Heat Mass Transfer* **8**, 1153–1169 (1965).
6. T. R. Johnson, Application of zone method of analysis to the calculations of heat transfer from luminous flame. Ph.D. thesis, Sheffield University (1971).
7. A. Lowe, T. F. Wall and I. McC. Stewart, I. A zoned heat transfer model of a large tangentially fired pulverized coal boiler, *Fourteenth Symposium (International) on Combustion*, pp. 1261–1270 (1974).
8. F. R. Steward and H. K. Guruz, Mathematical simulation of an industrial boiler by the zone method of analysis. In *Heat Transfer in Flames*, pp. 47–71 (1974).
9. G. R. Whitacre and R. A. McCann, Comparison of methods for the prediction of radiant heat flux distribution and temperature, ASME Paper No. 75-HT-9 (1975).
10. N. K. Nakra and T. F. Smith, Combined radiation-convection for real gas, *J. Heat Transfer* **99**, 60–65 (1977).
11. S. B. Gorrepati, Radiant exchange in a cylindrical enclosure with a participating media. M. S. thesis, Mechanical Engineering Program, University of Iowa (1978).
12. T. F. Smith and C. W. Clausen, Radiative and convective transfer for tube flow of a real gas, *Int. Heat Transfer Conference*, Vol. 3, pp. 391–396 (1978).
13. C. W. Clausen and T. F. Smith, Radiative and convective transfer for real gas flow through a tube with specified wall heat flux, *J. Heat Transfer* **101**, 376–378 (1979).
14. A. M. Alturki and T. F. Smith, Radiative and convective

- transfer for laminar flow of a gray gas in a cylindrical enclosure, TR-E-TFS-81-005, Division of Energy Engineering, University of Iowa (1981).
15. G. L. Badtram and T. F. Smith, Radiative and conductive transfer for a gray gas in a cylindrical enclosure with gray walls, TR-E-TFS-82-001, Division of Energy Engineering, University of Iowa (1982).
 16. T. F. Smith, Z. F. Shen and A. M. Alturki, Radiative and convective transfer in a cylindrical enclosure for a real gas, *J. Heat Transfer* **107**, 482–485 (1985).
 17. T. K. Kim, Radiative and conductive transfer for a real gas in a cylindrical enclosure with gray walls. Ph.D. thesis, University of Iowa (1984).
 18. T. F. Smith, T. K. Kim and Z. F. Shen, Evaluation of direct exchange areas for a cylindrical enclosure, TR-E-TFS-81-007, Division of Energy Engineering, University of Iowa (1981).
 19. T. F. Smith, Radiative exchange with the zone method, TR-E-TFS-81-008, Division of Energy Engineering, University of Iowa (1981).
 20. T. F. Smith, Z. F. Shen and J. N. Friedman, Evaluation of coefficients for the weighted sum of gray gases model, *J. Heat Transfer* **104**, 602–608 (1982).
 21. J. J. Noble, The zone method: explicit matrix relations for total exchange areas, *Int. J. Heat Mass Transfer* **18**, 261–269 (1975).
 22. Z. F. Shen, T. F. Smith and P. Hix, Linearization of the radiation term for improved convergence by use of the zone method, *Numer. Heat Transfer* **6**, 377–382 (1983).
 23. Manual for IMSL Library provided by the Weeg Computing Center at the University of Iowa.
 24. E. M. Sparrow and R. D. Cess, *Radiation Heat Transfer*. Hemisphere, Washington (1978).

TRANSFERT RADIATIF ET CONDUCTIF POUR UN GAZ REEL DANS UNE ENCEINTE CYLINDRIQUE A PAROIS GRISES

Résumé—L'objectif de cette étude est d'examiner l'interaction des transferts radiatif et conductif pour un gaz réel au repos et semi-transparent dans une enceinte cylindrique à parois grises. La considération de frontières réfléchissantes représente une extension d'études antérieures avec parois noires. Le transfert radiatif est considéré par la méthode des zones avec les propriétés du gaz données par la somme pondérée du modèle de plusieurs gaz gris. Les aires du flux directionnel sont exprimées comme la somme pondérée des aires totales d'échange du gaz gris qui sont évaluées par la méthode de formulation matricielle à partir des aires d'échange direct. Les températures du gaz sont considérées avec le flux ou la température à la paroi pour les cas respectifs soit de flux soit de température donnés sur la paroi. On discute les résultats pour montrer les effets de l'émissance pariétale et du diamètre du tube. On présente aussi des résultats pour la génération de chaleur dans le gaz.

WÄRMETRANSPORT DURCH STRAHLUNG UND LEITUNG FÜR EIN REALES GAS IN EINEM ZYLINDRISCHEN HOHLRAUM MIT GRAUEN WÄNDEN

Zusammenfassung—Zweck dieser Studie ist es, die Wechselwirkung von Wärmeübertragung durch Strahlung und Leitung für ein nicht diathermanes reales Gas, welches in einem zylindrischen Hohlraum mit grauen diffusen Wänden ruht, zu untersuchen. Die Berücksichtigung von reflektierenden Begrenzungen bedeutet eine Erweiterung von früheren Studien, bei denen von schwarzen Wänden ausgegangen wurde. Die Wärmeübertragung durch Strahlung wurde mit der Zonen-Methode unter Berücksichtigung der Eigenheiten der Gasstrahlung, welche über die gewichtete Summe von grauen Gasmodellen bestimmt wurde, untersucht. Die axiale und radiale Gas-Temperatur-Verteilung wurde in Abhängigkeit von der Wandwärmestromdichte oder der Temperatur untersucht, je nach dem, welche der Größen aufgeprägt war. Der Schwerpunkt wurde auf Untersuchungsergebnisse gelegt, welche die Einflüsse von Wandemission und Zylinderdurchmesser aufzeigen. Die Ergebnisse hinsichtlich der Wärmeerzeugung innerhalb des Gases werden ebenfalls präsentiert.

РАДИАЦИОННЫЙ И КОНДУКТИВНЫЙ ПЕРЕНОС ДЛЯ РЕАЛЬНЫХ ГАЗОВ В ЦИЛИНДРИЧЕСКИХ ЗАМКНУТЫХ ПОЛОСТЯХ С СЕРЫМИ СТЕНКАМИ

Аннотация—Цель работы—исследование взаимодействия радиационного и кондуктивного переноса для реального газа с радиационным переносом тепла, покоящегося в цилиндрической замкнутой полости с серыми диффузными стенками. Рассмотрение отражающих границ является продолжением ранее проводимых исследований черной стенки. Радиационный перенос изучался с помощью зонального метода, причем радиационные свойства газа были дополнены с помощью взвешенных сумм на основе модели серого газа. Зоны направленного потока выражены как взвешенные суммы зон полного обмена серого газа, которые оцениваются с помощью матричного метода по зонам прямого обмена. Аксиальные и радиальные температуры газа исследовались вместе с тепловым потоком у стенки и температурой, соответственно, как для случаев заданных температур, так и тепловых потоков. Особое внимание уделяется изучению влияния стенки и диаметра канала. Также представлены результаты по внутреннему тепловыделению в газе.